Expanded View Figures

Figure EV1. CAF-1 promotes HIV-1 latency.

A Mass spectrometry (MS) result of naïve and TNFα-stimulated J-Lat 10.6 cells. Significantly changed genes were plotted as heatmap. Representative genes were shown in table aside the heatmap. The heatmap scale represented fold change of gene expression (Min: −20 fold; Max: 20 fold).

B, C The GFP-positive percentages of heterogeneous sgCHAF1A and sgNT J-Lat 10.6 cell lines were shown as flow cytometry figure and statistical histogram. TNFα, SAHA and JQ-1 were used as supplements.

D Fifteen LRAs targeting eight signaling pathways were used in heterogeneous and homogeneous CHAF1A-KO J-Lat 10.6 cell lines.

E, F Two pseudotyped HIV-1 latency cell lines (J-Lat-NIB and J-Lat-NPB) were treated with sgCHAF1A lentiviruses, SAHA and JQ-1. The GFP-positive percentages of each group were measured. The backbones of each pseudotyped HIV-1 were also shown.

G–J J-Lat 6.3, 8.4, 9.2 and 15.4 were treated as in Fig 1C. The reactivation efficiencies of each group were indicated by the percentages of GFP-positive cells.

Data information: Data represented mean ± SEM in triplicate. *P*-values were calculated by Student's *t*-test. $*P < 0.05$, $**P < 0.01$, $***P < 0.001$.

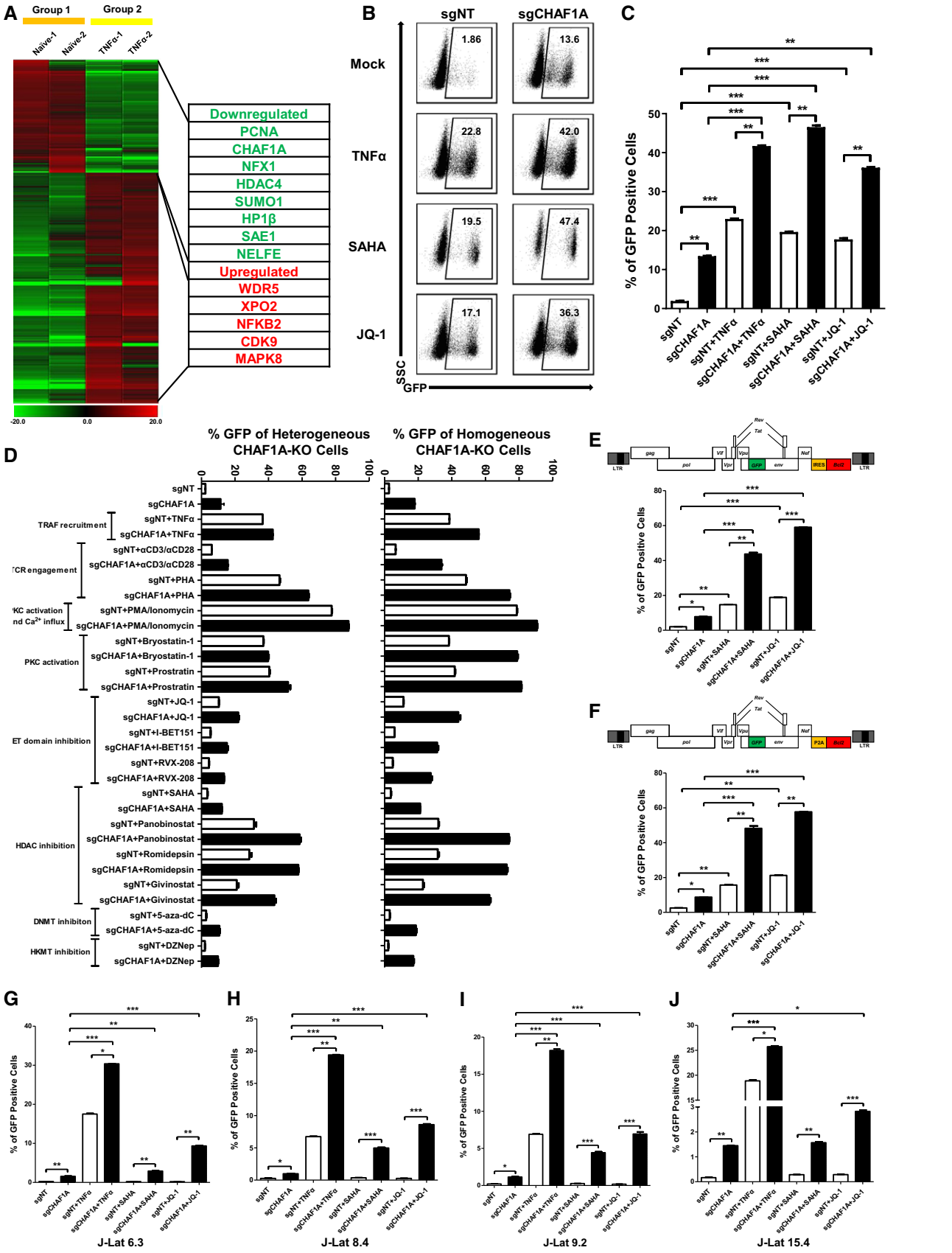

Figure EV1.

Figure EV2. CAF-1 alters the epigenetic status of HIV-1 promoter and enriches SUMOylation system.

A ChIP assay with antibody against CHAF1A was performed in TZM-bl cells as in Fig 1D. ChIP-qPCR DNA signals were normalized to Input. G5: cellular DNA and viral 5'LTR junction; L: luciferase region; G3: viral 3'LTR and cellular DNA junction. The other regions were as in Fig 1D.

B–E ChIP assays with antibodies against H3K9me, H3K9me2, H3K27me3 and H3K36me2 were performed as in Fig 1F.

F The schematic of CpGs on HIV-1 LTR of J-Lat 8.4. Eleven CpGs were shown in circles.

G, H The flow cytometry figures and Methyl-CpGs graphs of J-Lat 8.4 which were treated with shCHAF1A and 5-aza-dC, corresponding to statistical histograms in Fig 1J and K.

I RNA-Seq result of wild-type and CHAF1A-KO J-Lat 10.6. Differentially expressed genes were filtered with $\log_2$FC of 1 and *P*valueFDR cutoff of 0.05. Upregulated and downregulated genes were labeled as red and blue dots, respectively. Representative genes were labeled aside corresponding dots.

J Flag-tagged TRIM28, SUMO1, SUMO2 and SUMO4 were co-overexpressed with HA-tagged CHAF1A. HA-tagged CHAF1A was IP with anti-HA beads. Both total and IP samples were IB with anti-HA, anti-Flag and anti-Actin antibodies.

K HA-tagged CHAF1A and HA-tagged GFP were co-overexpressed with Flag-tagged CDK9. HA-tagged proteins were immunoprecipitated (IP) with anti-HA beads. Both total and IP samples were immunoblotted (IB) with anti-HA, anti-Flag and anti-GAPDH antibodies.

L HA-tagged CDK9 was co-overexpressed with Flag-tagged SUMO4, UBC9, and TRIM28. siRNAs targeting TRIM28 and CHAF1A treated CDK9-overexpressed HeLa cells, respectively. CDK9 was IP with anti-HA beads. Both total and IP samples were IB with anti-HA, anti-Flag and anti-GAPDH antibodies.

Data information: Data represented mean ± SEM in triplicate. *P*-values were calculated by Student's *t*-test. $*P < 0.05$, $**P < 0.01$, $***P < 0.001$.
Source data are available online for this figure.

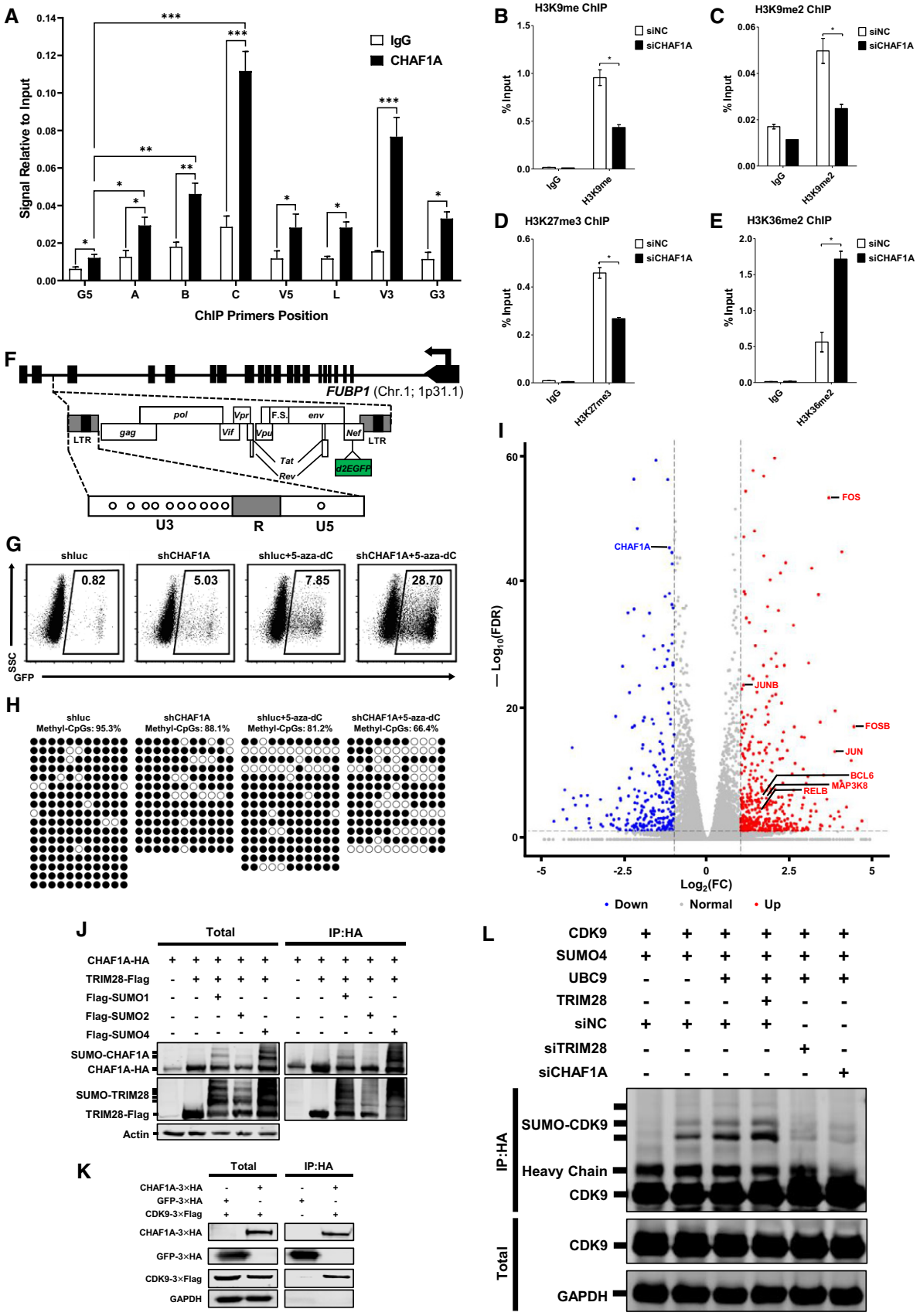

Figure EV2.

Figure EV3. CAF-1 forms nuclear bodies.

A GFP-tagged CHAF1A was imaged with AF594-tagged antibody against CHAF1A.
B RFP-tagged CHAF1A was imaged with AF488-tagged antibody against CHAF1A.
C, D The endogenous CHAF1A was imaged before (C) and after (D) CHAF1A knockdown in J-Lat 10.6 cells.
E, F Coilin and Pho-Ser5-RNAP II were immunostained with corresponding antibodies and imaged with CHAF1A, respectively.
G–L CHAF1B, RBBP4, PCNA, SUV39H2, HP1β, and HP1γ was co-overexpressed with CHAF1A, respectively. SIM images were captured for each combination.
M RFP-tagged PCNA and GFP-tagged DNMT1 were imaged with AF647-tagged antibody against CHAF1A simultaneously. DAPI was used to dye DNA.
N RFP-tagged HP1α, GFP-tagged DNMT1, and BFP-tagged PCNA were imaged with AF647-tagged antibody against CHAF1A simultaneously.
O–R CBX4, SUZ12, SUMO1, and SUMO2 were imaged with CHAF1A, respectively.

Data information: Scale bar represented 5 μm. At least three images were captured for each sample.

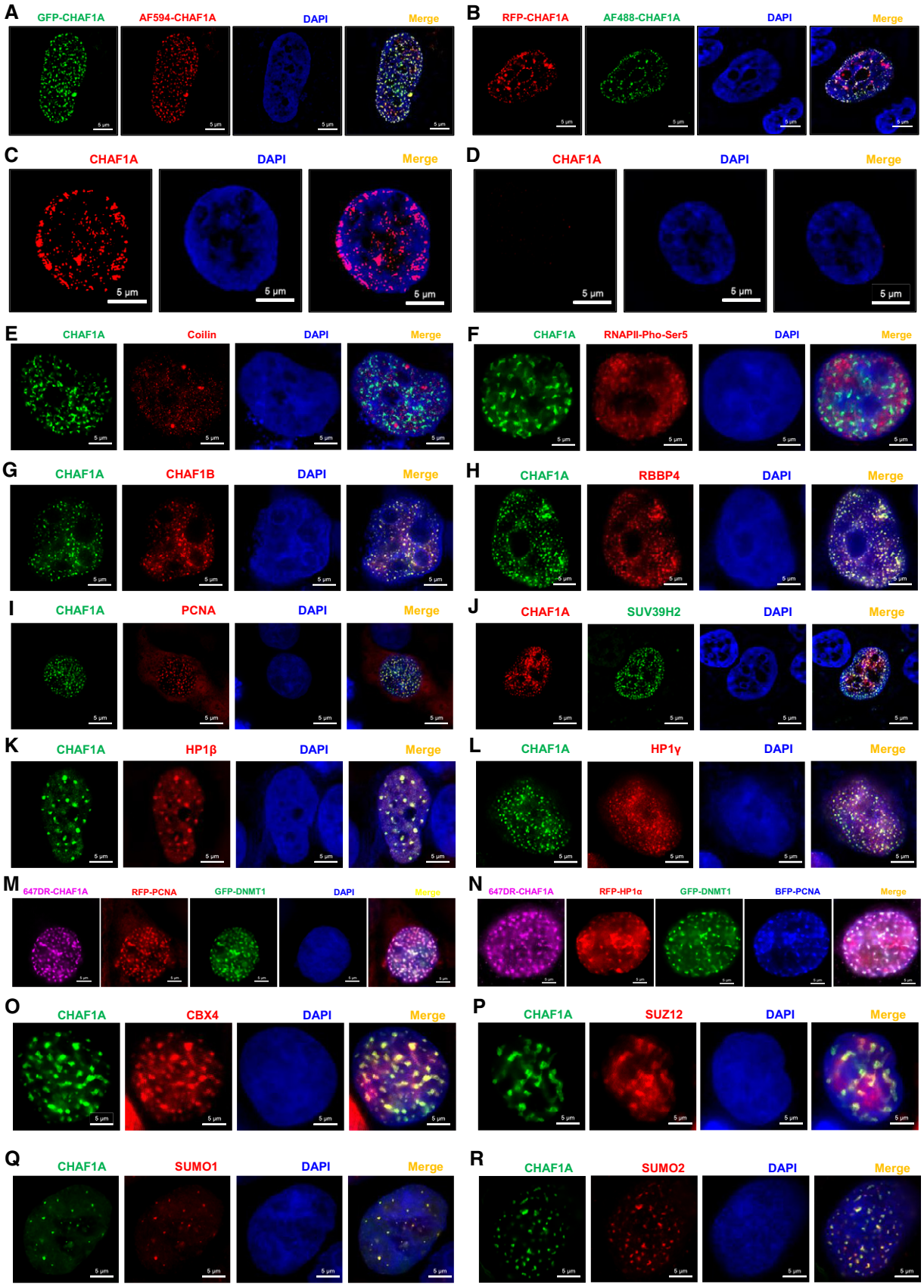

Figure EV3.

Figure EV4. The influence of different CHAF1A mutants on CAF-1 body and the epigenetic status of HIV-1 promoter.

A The distribution of CHAF1A-PIP2-C. PIP2: the second PCNA-interacting protein motif which located after KER. C: CHAF1A C-terminal.
B The co-localization of RFP-tagged SUMO1, SUMO2 and SUMO4 with GFP-tagged CHAF1A-dDS13.
C The distribution of CHAF1A-dDS13-dSIM.
D–F The enrichment of CHAF1A, H4K20me3 and H3K9Acetyl on HIV-1 LTR in different CHAF1A status.

Data information: The scale bar in (A–C) represented 5 μm. Data in (D–F) represented mean ± SEM in triplicate. *P*-values were calculated by Student's *t*-test. $*P < 0.05$, $**P < 0.01$.

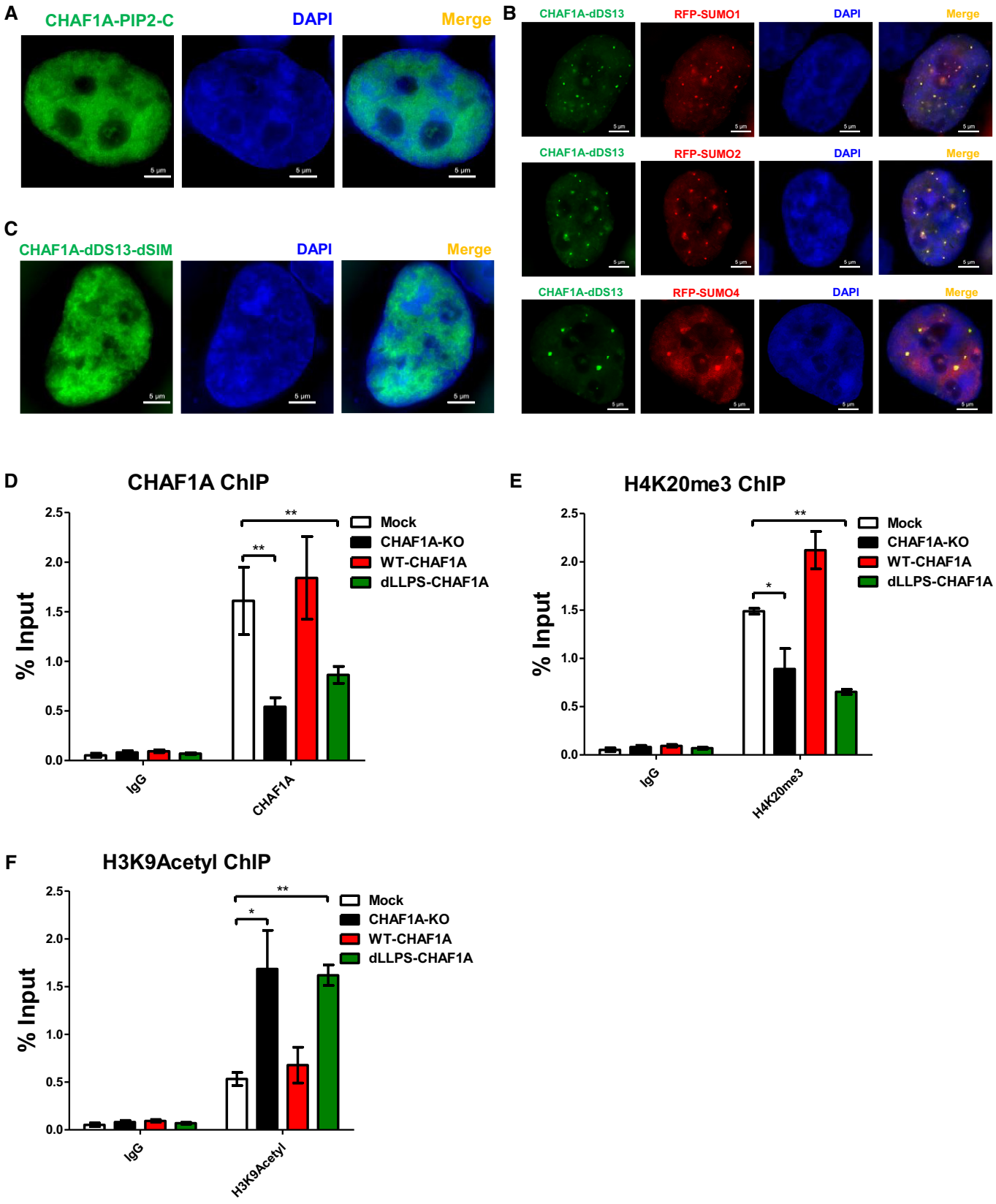

Figure EV4.

Figure EV5. CHAF1A depletion reactivates latent HIV-1 in primary CD4$^+$ T cells.

A The procedure of CHAF1A-mediated HIV-1 integration restriction. On Day −4, primary CD4$^+$ T cells were isolated from PBMCs of healthy donors, followed by the activation of PHA. On Day −2, endogenous CHAF1A was knocked down by shCHAF1A lentiviruses. Two days later, shluc- and shCHAF1A-treated cells were proceeded to the infection of pseudotyped HIV-1. Another 4 days later, the percentages of GFP-positive cells, which indicated the reactivation efficiency, were measured by FCM.

B The schematic of pseudotyped HIV-1 backbone used in (A).

C, D The FCM figures and statistical histogram of shluc- and shCHAF1A-treated groups.

E The procedure of CHAF1A-mediated delay of HIV-1 entering into latency. On Day −4, primary CD4$^+$ T cells were isolated and activated by PHA. On Day −2, activated CD4$^+$ T cells were washed and infected with pseudotyped HIV-1. Another 2 days later, cells were infected with shluc or shCHAF1A lentiviruses. In the following 2 weeks, the percentages of GFP-positive cells were measured by FCM every 4 days.

F The statistical histogram of the results in (E). Data showed results from three different healthy donors.

G The procedure of CHAF1A-mediated HIV-1 latency in wild-type HIV-1 latency model. The procedure was similar as in Fig 7A, except that the virus used in (G) was wild-type HIV-1 and the infected cells were treated with 5 μM AZT during the 2 weeks of resting status.

H The schematic of GFP-conjugated wild-type HIV-1 backbone used in (G).

I, J The representative FCM figures and statistical scatter plot of the results in (G).

Data information: Data in (D) represented mean ± SEM in triplicate. *P*-values were calculated by Student's *t*-test. Data in (J) represented mean ± SEM in sextuplicate. *P*-values were calculated by Mann–Whitney *U*-test. $*P < 0.05$, $**P < 0.01$.

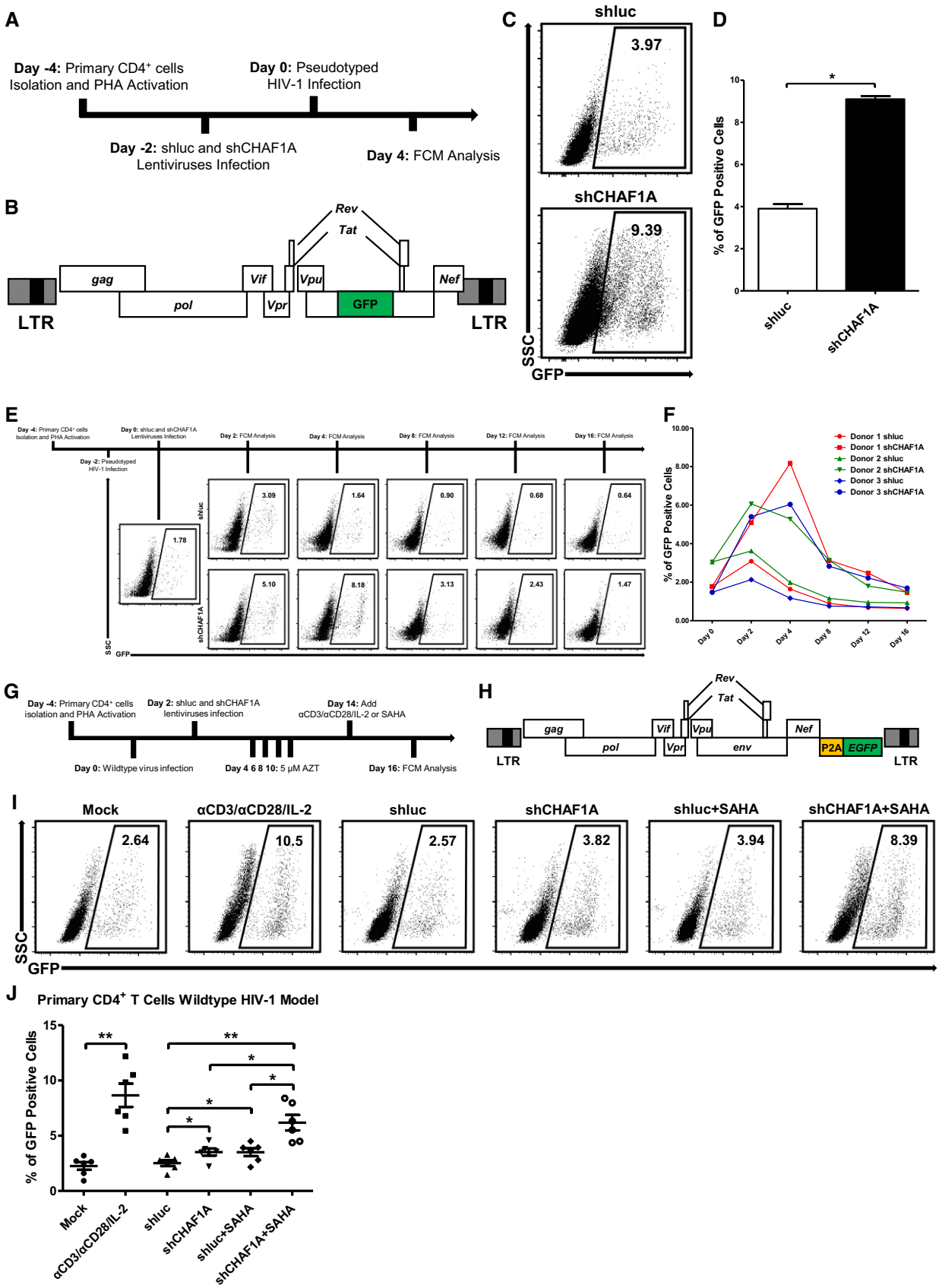

Figure EV5.